Numerical characterization of a new high-pressure multi-hole GDI injector

S. Malaguti*, S. Fontanesi, G. Cantore
* Dipartimento di Ingegneria Meccanica e Civile
Università degli Studi di Modena e Reggio Emilia
Modena, 41125 Italy

Abstract

The paper reports a numerical activity aiming at investigating the spray structure originated by a new-generation multi-hole GDI injector. The spray is analyzed under quiescent conditions, injecting the fuel in a test vessel at non-evaporative ambient conditions [1].
Results from 3D-CFD simulations are compared to experimental measurements available in literature, in which commercial gasoline at two different injection pressures (10 and 20 MPa) was injected and the spray evolution was analyzed throughout the injection duration. The spray was investigated along the jet axis by phase Doppler anemometry in order to provide droplet size and velocity, in terms of both axial and radial components.
Experimental measurements briefly described above are used to test and validate some lagrangian spray numerical sub-models and numerical parameters such as grid density, numerical setup, primary and secondary fuel breakup and droplet to droplet interaction. Particular care is devoted to the accurate representation of the spray primary breakup, in view of the lack of ad-hoc developed models available in literature. A wide CFD activity is then performed in order to correctly predict both liquid spray penetration and droplet size.
Results from the CFD analyses show a relevant dependency of the spray structure on the adopted CFD model ensemble.

Introduction

Second generation of high-pressure GDI injectors is characterized by a non-axisymmetric multi-hole architecture aiming at optimizing fuel-air mixing and fuel vapor diffusion through the combustion chamber. Figure 1 shows the 6-hole GDI injector investigated in the present paper, which is characterized by a nominal injection pressure of 150 bar. A sketch of the nozzle tip is reported in Figure 1, while Figure 2 shows the characteristic spray pattern. A strong interaction between each single jet is expected from this non-axisymmetric configuration and is confirmed from experimental spray images available in literature [1].

First generation multi-hole injectors, which are characterized by an axisymmetric jet spacing, have been widely investigated, and experimental data are available in literature [2, 3] for different nozzle configurations and hole spatial distributions, aiming at promoting and maximing mixture formation [4].

Compared to first generation multi-hole GDI injectors, the specific hole distribution and orientation causes a different jet to jet interaction for each single jet, strongly dependent on the single jet position relative to the overall spray. Furthermore, since the injector, which is analyzed in the present paper is characterized by a relatively low overall cone angle amplitude (< 90 degrees), the resulting spray structure appears to be narrow and single jets are not clearly distinguishable. As a result, a clear understanding of the mutual jet influence is far from being trivial.

Since spray morphology and its interaction with the surrounding air are strongly dependent on the specific hole distribution, second generation non-axisymmetric injectors is still an open challenge. In fact, despite the above described particular spray structure and its interaction with the combustion chamber walls are specifically designed to meet proper fuel-air distribution over a wide range of injection pressures and engine operating conditions, both design and operation effects on the resulting spray patterns are difficult to be generalized.

A deep and accurate understanding of the spray behavior and morphology is therefore mandatory, since fuel spray structure is widely recognized to play a dominant role on the subsequent mixture formation, ignition, combustion and pollutant formation [5].

An exhaustive experimental characterization of the broad range of injector designs and operating conditions is extremely complex and far from being feasible from an industrial viewpoint and the use of numerical simulations can be extremely proficient; in view of the lack of wide recognized numerical procedure, a wide CFD campaign is carried out to investigate the spray behavior in terms of both pointwise and global parameters.

* Corresponding author: simone.malaguti@unimore.it

Nozzle and injector characteristics

As stated earlier, CFD analyses are performed for the gasoline spray generated by a second generation multi-hole GDI injector characterized by a nominal injection pressure of 150 bar.

Due to the well known influences of both the injection pressure and ambient conditions on the resulting spray morphology, two different injection pressures are simulated in the present paper, i.e. 10 MPa and 20 MPa respectively.

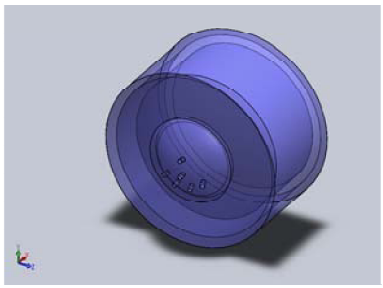

Figure 1. Injector tip

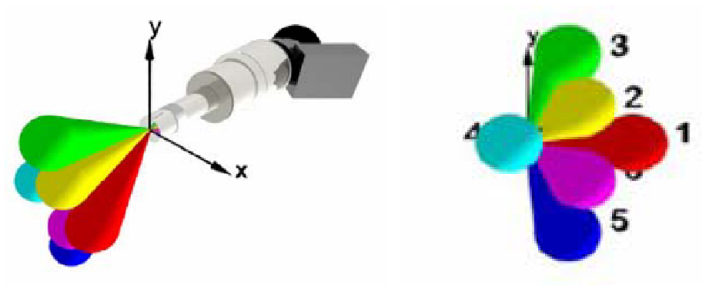

Figure 2. Jet spatial distribution

Figure 3 summarizes all the other injector characteristics. A beam angle equal to 17° is derived from injector specifications by the injection system manufacturer, despite Allocca et al. reports a smaller angle (12°) from experiments on the same injector [1].

Concerning the injector flow rate, measured instantaneous profile is adopted in order to properly take into account dynamic effects at the beginning of the injection process. In fact, despite standard CFD practice usually refers to simplified injection profiles accounting for the sole steady part of the injection, the actual injection profile is relevantly influenced by dynamic effects within the injection system. The flat portion of the injection profile suggests that a discharge coefficient ranging between 0.6 and 0.7 characterizes the injector for both the injection pressures.

Hole Number	6	
Nominal Cone angle	60	[°]
Single Beam Angle	17	[°]
Injection Pressure	100, 200	[bar]
Back Pressure	1	[bar]
Injection Duration	1.5, 2.6	[ms]
Fuel Gasoline	750	[Kg/m3]

Figure 3. Injector characteristics

CFD set up

Grid

A grid of regularly-shaped hexahedral cells is generated to mimic the test vessel used in [1], in order to maximize cell quality and therefore minimize the effects of cell topology on the accuracy of the numerical forecasts. The grid is generated by means of the uniform extrusion of a "butterfly"-shaped set of 2-D shells giving rise to cells of approximately 1.0×1.0×1.0 mm^3 at the injector.

As a preliminary step, three additional grids are compared to the one described before, in order to quantify the effect of grid size on the CFD results. Both the second and the third grid are once again uniform extrusions where the cell size increases to 1.5 and 2.0 mm respectively, while the fourth grid is a the result of a non-uniform extrusion of the shells originating grid 1, where a stretch factor is applied to progressively coarsen the grid moving away from the injector.

Numerical Model

CFD calculations are performed using the three dimensional code Star-CD [6,7] by CD-Adapco. The vessel is simulated adopting fixed wall temperature, while quiescent air thermo physical properties are computed as a function of local temperature and pressure conditions [8]. Turbulence is modeled adopting the RNG k-□. model, as implemented by Yakhot et Al. [9]. Concerning the injected fuel, a coupled lagrangian approach is used within the Star-CD code [10, 11]. Numerical sub-models accounting for turbulent dispersion [12], condensation and collision [13] are adopted. Finally, droplet thermo physical properties are temperature dependent.

Primary breakup

Concerning the atomization process, Reitz's approach [14, 15], also known as "Blob" model, is at first used. According to the model, all the injected droplets have the same radius as the nozzle exit hole radius. The initial axial velocity component of the fuel droplets is given by

$$V_0 = C_d (2\Delta P/\rho_l)^{1/2} \tag{1}$$

where C_d is the nozzle discharge coefficient, ΔP is the injection pressure gauge and ρ_l is the liquid density. The radial velocity component is

$$V_r = V_0 \tan\left(\frac{\Theta}{2}\right) = V_0 A \left(\frac{\rho}{\rho_l}\right)^{1/2} \tag{2}$$

where Θ is function of the cone angle, ρ is the gas density, and A is a constant dependent on the specific nozzle design.

In order to improve the CFD results and properly predict the initial droplet distribution at the nozzle exit, Huh-Gosman atomization model [16, 17] is also used and compared to Reitz's model. As in the Kelvin-Helmholtz model, this approach assumes that as the liquid emerges from the nozzle an unstable surface wave forms, grows and breaks up with characteristic atomization length scale L_A and time scale τ_A. This process erodes the inner liquid core until complete atomization occurs. The model takes into account the effect of turbulence assuming L_A proportional to the turbulence length scale L_t and τ_A as a linear combination of the turbulence time scale τ_t and the wave growth time scale τ_w.

Secondary droplet breakup

As far as droplet breakup is concerned, the model by Reitz and Diwakar [14, 15] is at first applied for the GDI spray simulation. According to the model, droplet breakup due to aerodynamic forces occurs in one of the following modes:

1. "Bag" breakup, in which the non-uniform pressure field around the droplet is taken in account and the following breakup criteria must be met for each computational parcel at each time step;

$$We \equiv \frac{\rho |u - u_d^2| D_d}{2\sigma_d} \geq C_{bl} \tag{3}$$

$$\tau_{bl} = \frac{C_{b2} \rho_d^{1/2} D_d^{3/2}}{4\sigma_d^{1/2}} \tag{4}$$

2. "Strip" breakup, in which liquid is sheared or stripped from droplets surface. To determine strip breakup criteria equations (5) and (6) are assumed:

$$\frac{We}{\sqrt{Re_d}} \geq C_{s1} \tag{5}$$

$$\tau_b = \frac{C_{s2}}{2}\left(\frac{\rho_d}{\rho}\right)^{1/2} \frac{D_d}{|u - u_d|} \tag{6}$$

where u is the gas velocity, u_d is the liquid velocity, D_d is the droplet's diameter, σ_d is the surface tension of the liquid, We is the Weber number and Re_d is the Reynolds number.

Results and Discussion

Grid Dependence

In this section, results from CFD simulations are compared to experimental data in literature in terms of both spray penetration and droplet mean diameters (D_{10}). Measurement sections by means of PDA technique focus on one of the six jets, i.e. jet number 4, at three distances ranging from 10 to 30 mm from the injector tip, as visible in Figure 4 below.

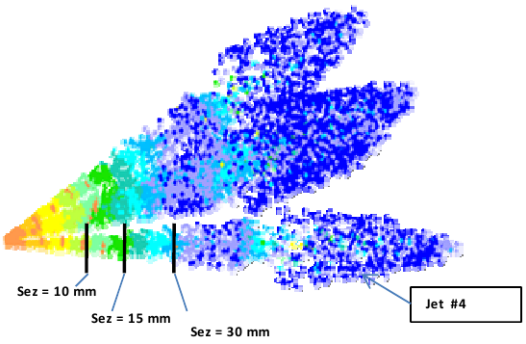

Figure 4. Sketch of the measurement sections

The four grids described earlier are tested adopting the same numerical setup, i.e. the "Blob model" approach for the atomization process and Reitz-Diwakar's model [15] for the secondary breakup. Figure 5 reports jet 4 tip penetration for the two injection pressure conditions and the four computational grids described above.

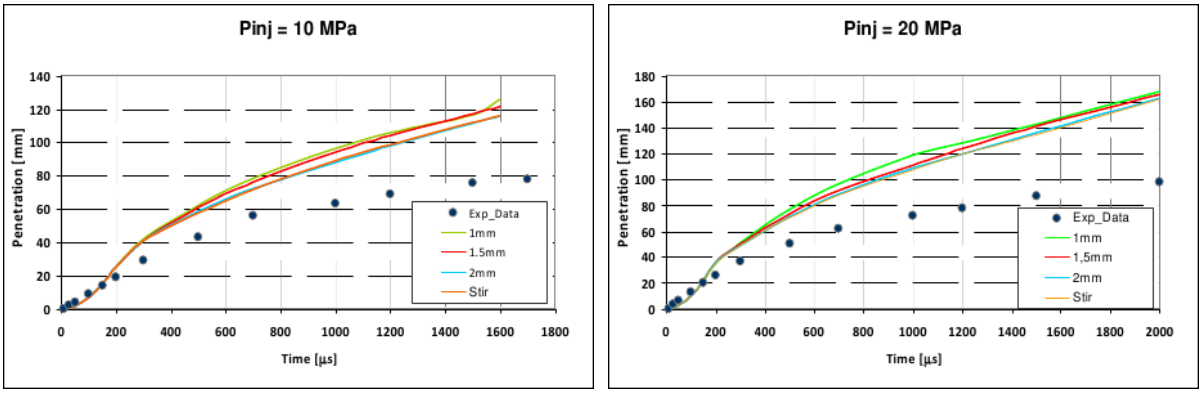

Figure 5. Tip penetration comparison 100 bar injection pressure

Figure 5 highlights that droplet drag coefficient estimation is only slightly dependent on cell size at least for average internal combustion engine grid spacing. It is worthwhile to remark that the comparison against experimental evidence is carried out using Star-CD's default settings for droplet breakup which will be strongly revised in the subsequent section, and results are analyzed without stressing the attention on the relevant tip penetration overprediction.

Although a coarsening of the computational grid allows a larger population of parcels to undergo the same high drag resistance of the forefront droplets, even the coarsest grid proves to be unable to radically improve the CFD representation of the actual spray behavior. Since a further increase in the computational cell size would be detrimental for the correct estimation of both the spray/spray and spray/air shear effects, an improvement in the accuracy of the CFD simulations cannot be demanded to grid spacing. A further analysis of these preliminary simulations shows that droplet diameters are strongly overpredicted for all the three measurement sections, this explaining the higher tip penetration visible above.

A substantial improvement must necessarily be found in the modeling of both fuel atomization and droplet breakup.

Concerning secondary breakup, Figure 6 below shows the effects of the tuning process of Reitz's model bag and strip breakup constants for the 10 MPa injection pressure. Results from this set of simulations clearly indicate that decreasing the values of the C_{b1} and C_{s2} constants (see Blob_Bre1, green line), while keeping unaltered the other model constants, as literature suggests [15], lead to a non negligible improvement in terms of spray penetration prediction. Despite the good agreement between numerical forecasts and experimental evidence in terms of spray tip penetration, sections 15mm and 30mm show higher droplets diameters. To improve results in terms of average droplet size, modifications of C_{b2} and C_{s1} constants are then superimposed (see Blob_Bre2, red line). As visible, satisfactory results in terms of both penetration and droplet size can be achieved if proper tuning is adopted, although a non negligible overestimation in terms of D_{10} is still visible at section 30mm.

The same set of optimized model constants is then applied to different injection conditions, i.e. an injection pressure of 20 MPa, in order to see whether the above CFD setup can be generalized or not. Results reported in Figure 7 clearly indicate that a good agreement in terms of spray penetration can be found only at the very beginning of the injection process, i.e. from injector opening to 1 ms, while an increasing overestimation of the spray penetration is found for the remaining of the injection. Combining this observation to the analysis of droplet size,

which shows a non negligible underestimation of mean droplet diameter, it is possible to state that the strong underprediction of droplet momentum decay is mainly due to an increasing overestimation of droplet velocity. In order to see whether a change in spray behavior can be found by means of a different atomization treatment, results from the optimized blob model (see Blob_Bre2, red line) are then compared to those from the Huh-Gosman atomization (see Huh_Default, light blue line).

Results from this further comparison show that the adoption of the Huh-Gosman atomization model, without any tuning of the model constants, leads again to a slight overestimation of spray penetration. Information from droplet size evolution through the three measurement sections appears to be confusing, since D_{10} is initially underpredicted, mainly by the atomization model itself, at the test section closest to the injector tip, while it slightly grows moving to the following sections without properly taking into account secondary breakup effects.

It is worthwhile to remark that slight differences exist in the evaluation of D_{10} between CFD practice and experiments, which could partially explain the differences stated above. In fact, experimental D_{10} refers to jet 4 droplets along the jet axis, while CFD refers to the average diameter for the whole jet 4 section at the given distances from the injector tip.

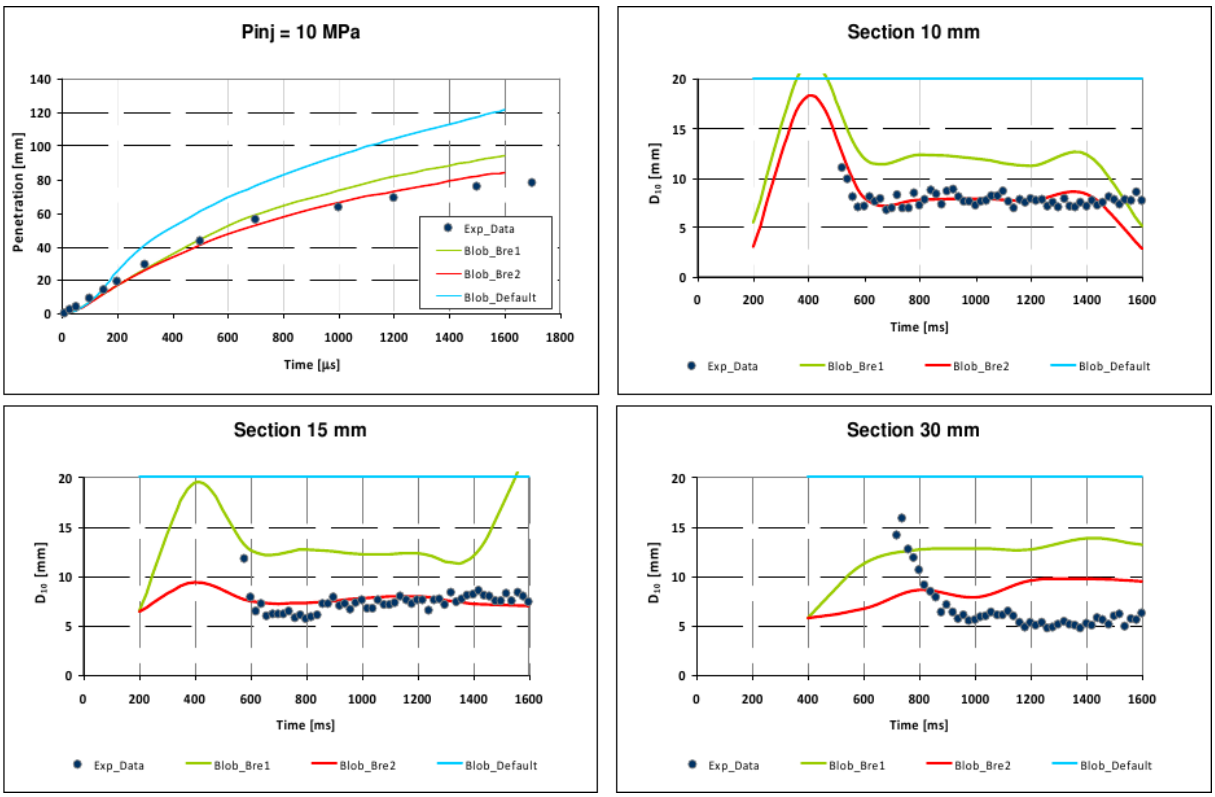

Figure 6. Comparison between CFD and experiments - 10 MPa injection pressure

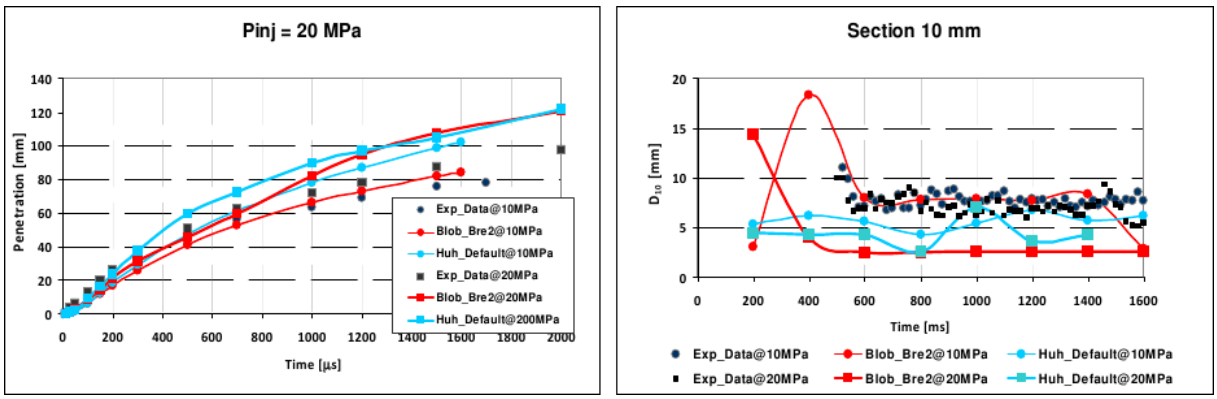

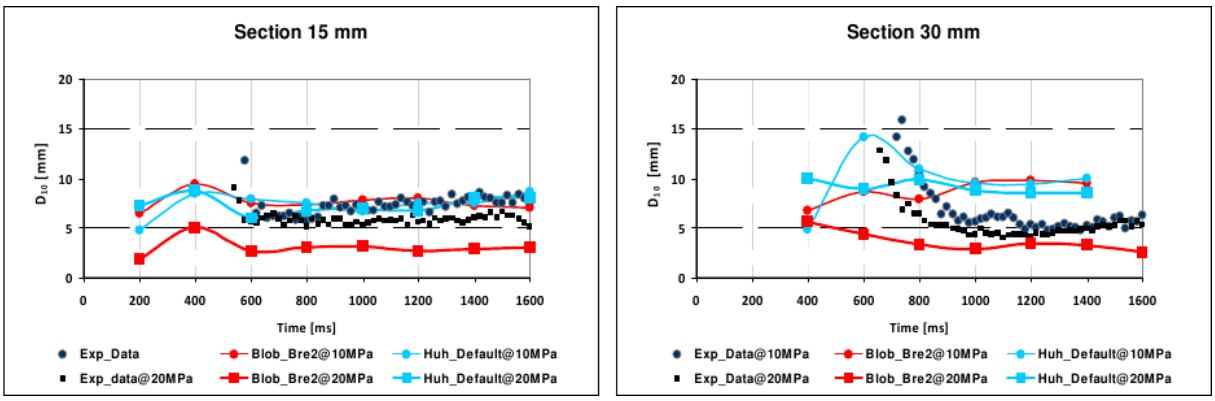

Figure 7. Comparison between CFD and experiments – 10 MPa and 20 MPa injection pressure

In order to better understand the above described behavior for the different tested models and to address further improvements to the CFD methodology, the resulting sprays are deeply analyzed and investigated in terms of spatial morphology and temporal evolution, once again by means of the comparison with experiments in terms of spray visualization throughout the injection process.
Figure 8 below clearly shows that both the tuned Blob model and the Huh-Gosman one lead to a spray morphology where the jet to jet interaction is strongly overestimated: in fact, outer sprays 1, 3, 4, 5 are those initially undergoing the highest aerodynamic impact with the surrounding air, and give rise to a low-pressure region in the spray inner region. The major consequences of this behavior are:

- inner jets 2 and 6 meet lower levels of drag resistance during the first part of the injection, and are characterized by axial velocities almost 30% higher than the outer jets' (see Figure 9 below, where the different jet velocity is shown for the 10 MPa injection pressure);
- outer jets get deviated by the low-pressure region at the spray core, and the resulting overall spray angle appears to be narrower than the actual one, as visible from the observation of Figure 10 below, where the outer jet deviation is highlighted;
- when inner jet droplets overcome, in view of their higher velocity, those from the outer jets, the strong impact against the air at the forefront deviates them towards the spray outer region, strongly enhancing the interaction between the inner and the outer jets, which are now relevantly deviated towards the outside by the core droplet trajectory, as visible in Figure 11 below, where the distortion of outer jet velocity field is reported.

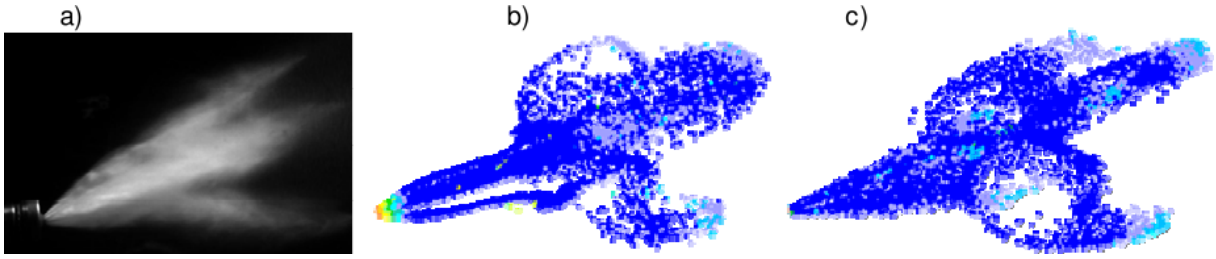

Figure 8. Simulations vs. experiments @700 μs: a)Experimental; b) Blob_Bre2; c)Huh_Default

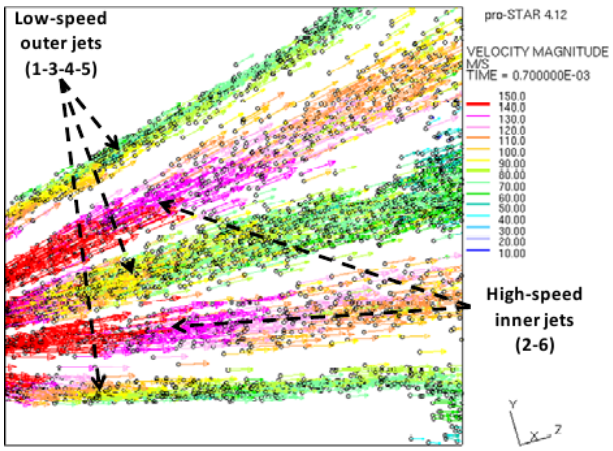

Figure 9. Sketch of the velocity vectors of the droplets @ 700 µm

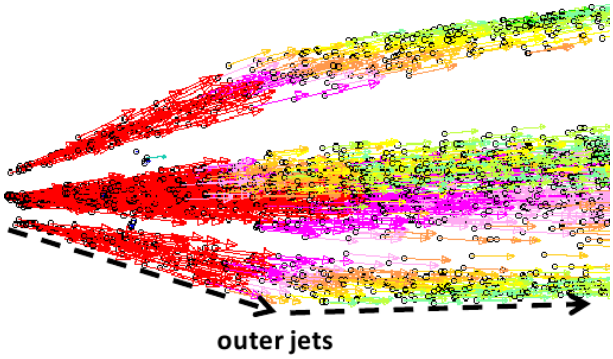

Figure 10. Deviation of the outer jets @ 700 µm

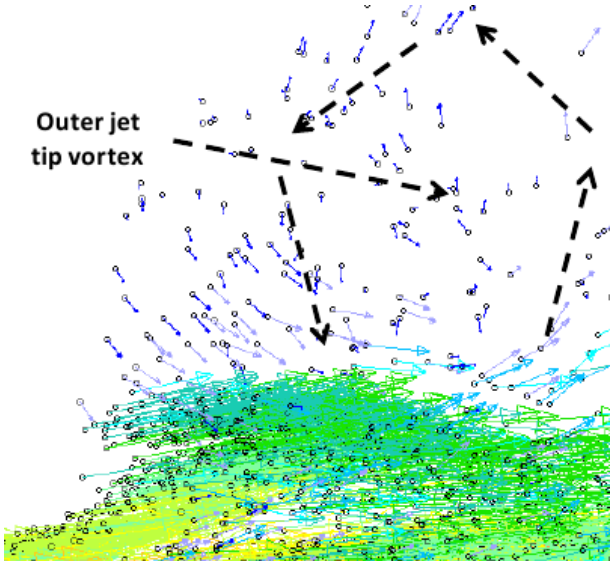

Figure 11. Outer jets tip vortex recirculation

As a results, it is possible to state that neither the Blob nor the Huh-Gosman atomization model are capable of correctly reproducing the multi-hole spray morphology investigated in the present paper. Despite the two CFD setup lead to similar results, some relevant differences can be observed: on one hand, the Blob simulation produces very big droplets at the injector outlet, which are quickly disintegrated into small droplets by the effects of the secondary breakup enhancement to match the experimental measurements. On the other hand, the Huh-Gosman simulation produces very small droplets by the primary breakup itself, giving rise to droplet diameters of nearly 11 µm just at the end of the atomization process. As a consequence, secondary breakup must be limited in

order to avoid excessive droplet disintegration leading to a mismatch between numerical forecasts and experiments.

For this reason, no further model constant tuning is reported in the paper, since a substantial modification to the modeling approach appears to be recommendable.

The last set of simulations is therefore carried out aiming at improving the above results, and is based on the "artificial" introduction of atomized droplets at a given distance from the injector tip, in order to completely bypass the atomization models described earlier. An ad-hoc user subroutine is therefore implemented based on the following assumptions:

- droplet diameters resulting from liquid atomization are set by means of a Rosin-Rammler distribution, whose average diameter is computed in order to match experimental penetration and size;
- droplets are inserted at a distance from the injector tip based on results from the Huh-Gosman atomization model;
- droplet velocity is derived from the experimental flow rate accounting for the injector discharge coefficient;
- droplet angle varies by means of a random function ranging between zero degrees (i.e., axial velocity only) and the experimentally measured angle.

Concerning secondary breakup, Reitz-Diwakar's model is used, where a slight tuning of C_{b1} and C_{s2} constants is adopted with reference to the standard range [15]. No additional modification to the standard values of the remaining model constants, i.e. C_{b2} and C_{s1}, is required in order to match the experimental measurements. It is important to remark that this approach is, as expected, strongly dependent on the choice of a proper diameter for the inserted droplets, i.e. those resulting from the liquid atomization. Different diameter distributions were therefore preliminarily tested, and the resulting distribution, whose average D_{10} diameter is approximately 50 μm, falls in between those originated by the different atomization models described earlier, i.e. the big droplets by the Blob model and the small ones by the Huh-Gosman's model.

Results from this last set of simulations are reported in Figures 12 and 13 here below, where the advantages brought in by the insertion of a "properly atomized" set of droplets appear clearly visible.

The CFD forecasts, in fact, are able to correctly predict both spray tip penetration and droplet size evolution, and the resulting spray morphology matches experimental images.

The good correspondence between predicted and measured data confirms that liquid atomization at the injector outlet plays a dominant role on the subsequent spray evolution.

In fact, although penetration and D_{10} can be matched by means of "standard" atomization models (available in literature and mostly derived from Diesel injection) [14, 15, 16, 17] through a proper tuning of the different model constants, spray behavior and subsequent spray morphology can result relevantly different from experimental visualization.

Conversely, the adopted modeling strategy, i.e. the complete substitution of any atomization model by means of the insertion of artificially atomized droplets, leads to a fully consistent prediction of the spray behavior. Since the process requires an ad-hoc definition of the inserted droplets, general relationships between droplet characteristics and injection parameters would be highly recommendable, in order to avoid or even completely avoid manual intervention.

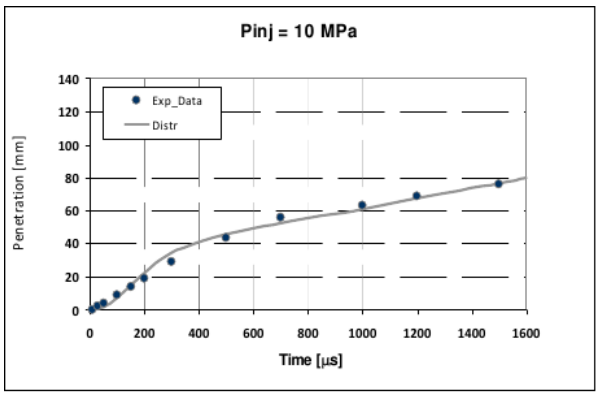

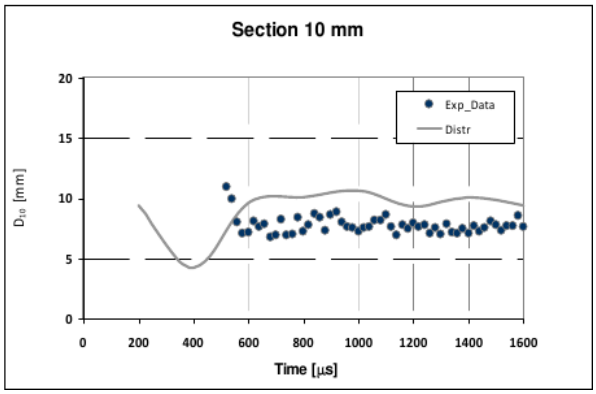

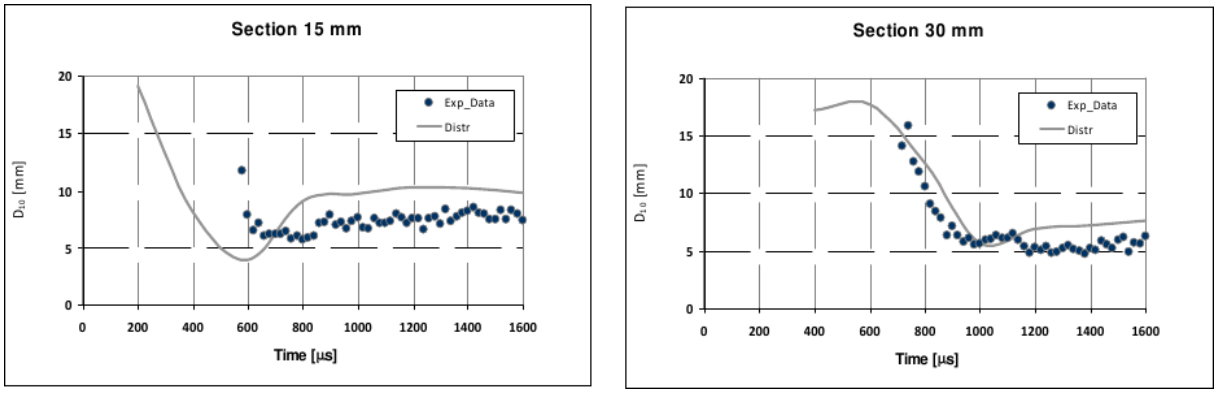

Figure 12. Comparison between CFD and experiments - 10 MPa injection pressure

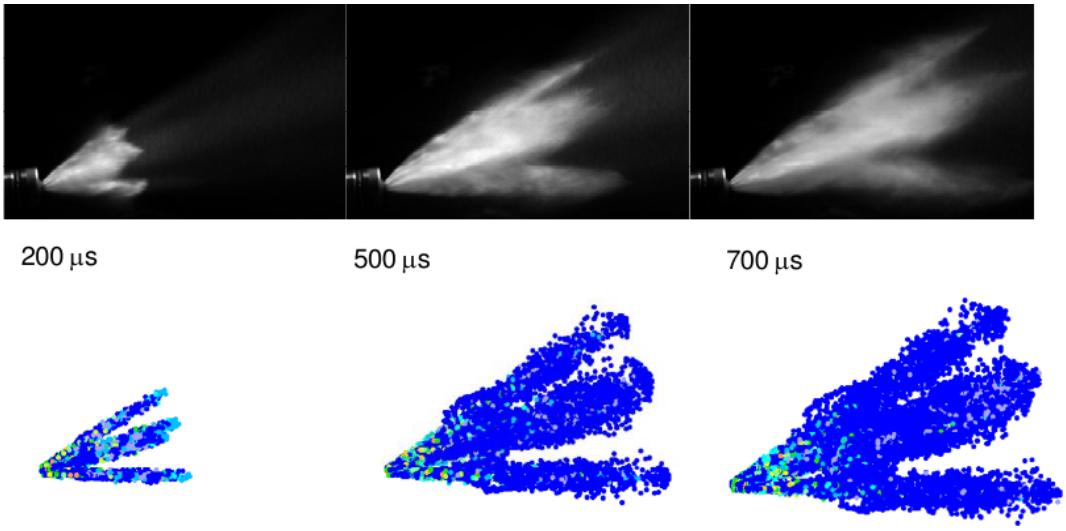

Figure 13.

Conclusions

The paper reports the CFD analysis of a second generation multi-hole GDI injector characterized by a non-axisymmetric hole distribution at the nozzle. 3D-CFD simulations are carried out within the framework of the lagrangian approach to the modeling of fuel sprays. In view of the spatial complexity of the actual injector, results from the full 6-hole injector are deeply analyzed in terms of both global parameters and pointwise fuel droplet distribution and properties.

A sensitivity analysis is at first performed on grid size, which is known to influence the estimation of droplet drag coefficient. Relevant discrepancies between CFD forecasts and measurements show that a proper matching cannot be demanded to grid size and spray sub-models must be investigated.

As a second step, therefore, different primary break-up models available in literature are tested and evaluated. Even if the above process is carried out iteratively in combination with a wide activity on the tuning of droplet secondary break-up Reitz-Diwakar model's constants, both Blob and Huh-Gosman primary break-up models show some inadequacies in correctly capturing the global spray behavior.

Despite the two atomization models lead to similar results, some relevant differences can be observed in terms of primary and secondary breakup contributions to the overall process: on one hand, within the Blob framework, droplet disintegration is demanded to secondary breakup, whose effect must be adequately enhanced to match the experimental measurements. On the other hand, the Huh-Gosman simulation produces very small droplets by the primary breakup itself, and secondary breakup must be limited in order to avoid excessive droplet disintegration.

Since neither of the two atomization models appear to be capable of correctly capturing the spray morphology, which is the result of different jet to jet interactions caused by the non axisymmetric hole distribution, a user-implemented routine is tested aiming at manually specifying droplet initial conditions at the injector holes, therefore avoiding primary break-up model deficiencies. Different droplet distributions are analyzed, showing

promising results in terms of both pointwise and global spray parameters. Despite the proposed procedure lacks of generality, results are useful to highlight the responsibility of different physical phenomena on the above mentioned deficiencies of the tested primary break-up models for the particular class of GDI injectors.

References

[1] L. Allocca, S. Alfuso, L. Marchitto, G. Valentino, "GDI Multi-Hole Injector: Particle Size and Velocity Distribution for Single and Jet-to-Jet", ICLASS, 2009.
[2] N. Mitroglou, J. M. Nouri, M. Gavaises and C. Arcoumanis, "Spray characteristics of a multi-hole injector for direct-injection gasoline engines", Int. J. Engine Research, 2005.
[3] S. Tonini, M. Gavaises, C. Arcoumanis, G. E. Coassali, M. Marengo, "Modelling of spray characteristics from multihole-hole injectors for gasoline engines" ICLASS paper, iclass06-06-239, 2006.
[4] N. Mitroglou, J.M. Nouri, Y.Yan, M. Gavaises and C. Arcoumanis, "Spray structure generated by multihole injectors for gasoline direct-injection engines" SAE Technical Paper, 2007-01-1417, 2007.
[5] Fuquan Zhao, "Automotive gasoline direct injection Engines (SAE)", 2002.
[6] Computational Dynamics, "STAR-CD User Guide", 2004, London (UK).
[7] Computational Dynamics, "STAR-CD Methodology", 2004, London (UK).
[8] S. Fontanesi, V. Gagliardi, S. Malaguti, G.Valentino, M. Auriemma "Detailed experimental and numerical investigation of the spry structure in a GDI high-pressure swirl injector", ICLASS paper,Kyoto,2006.
[9] Yakhot, V., Orszag, S.A., Thangam, S., Gatski, T.B., and Speziale, C.G.. "Development of turbulence models for shear flows by a double expansion technique", *Phys. Fluids*, 1992.
[10] N. Dombrowski, W. R. Johns, " The aerodynamic instability and disintegration of viscous liquid sheets", Chem. Eng. Sci., v. 18, p. 203, 1963.
[11] R.D. Reitz, F.V. Bracco, "Mechanism of Atomization of a Liquid Jet", Phy. Fluids, Vol. 25, ch. 10, Oct., 1982.
[12] Gosman, A.D., and Ioannides, S.I., 'Aspects of computer simulation of liquid-fuelled combustors', *AIAA*, *J. Energy*, **7,**1983.
[13] O'Rourke, P.J. "Collective Drop Effects on Vaporising Liquid Sprays". PhD Thesis, University of Princeton, 1981.
[14] Reitz, R.D., and Diwakar, R. 1986. "Effect of drop breakup on fuel sprays", SAE Technical Paper Series 860469.
[15] Reitz, R.D., and Diwakar, R. 1987. "Structure of high-pressure fuel spray", SAE Technical Paper Series 870598.
[16] Huh, K.Y., and Gosman, A.D. 1991. 'A phenomenological model of Diesel spray atomisation', Proc. Int. Conf. on Multiphase Flows, (ICMF '91).
[17] Kang Y. Huh, Eunju Lee, "Diesel spray atomization model considering nozzle exit turbulence conditions" , Atomization amd Sparys, vol. 8, 1998.
[18] S. Malaguti, S. Fontanesi, G. Cantore, Università di Modena e Reggio Emilia, A. Rosetti, R. Lupi, [Fiat Powertrain Technologies] "CFD investigation of wall wetting in a GDI engine under low temperature cranking operations", SAE Paper 2009-01-0704, 2009.
[19] Lefebvre, A. H., Atomization and Sprays, Hemisphere Publishing Corp., 1989.